The effect of grain orientation on the morphological stability of the organic–inorganic perovskite films under elevated temperature*

Dong Wang, Yue Chang, Shuping Pang†, and Guanglei Cui†

Qingdao Institute of Bioenergy and Bioprocess Technology, Chinese Academy of Sciences, Qingdao 266101, China

Abstract: The fast developing perovskite solar cells shows high efficiency and low cost. However, the stability problem restricts perovskite from commercial use. In this work, we have studied the effect of grain orientation on the morphological stability of perovskite thin films. By tuning the inorganic/organic ratio in the precursor solution, perovskite thin films with both high crystallinity and good morphological stability have been fabricated. The thermal stability of perovskite solar cells based on the optimized films has been tested. The device performance shows no degradation after annealing at 100 ℃ for 5 h in air. This finding provides general guidelines for the development of thermally stable perovskite solar cells.

Key words: perovskite solar cells; morphological stability; grain orientation

DOI: 10.1088/1674-4926/38/1/014002 **PACS:** 81.15.-z ; 81.07.Pr **EEACC:** 4200; 4250

1. Introduction

The novel hybrid organic–inorganic solar cell based on trihalide perovskite has attracted much attention due to its unique optical/electrical properties, such as intense light absorption, decent ambipolar carrier mobility, and long carrier lifetime[1−4]. The power conversion efficiency of perovskite solar cells (PSCs) have boosted over 20% in seven years[5]. Although the fast developing PSCs show both high efficiency and low cost, the stability issue of perovskite solar cells, including chemical stability and thermal stability, should be solved before its industrialization. As the encapsulation technology can efficiently isolate perovskite from the outside environment, the chemical stability of perovskite is well solved[6, 7]. The challenge facing the PSCs is thermal stability. Although the commonly used perovskite powder material is stable below 300 ℃[8−10], the thermal stability is largely reduced when thin perovskite film is deposited in the porous TiO_2 scaffold or on the compact TiO_2 film[11, 12]. Most importantly, beside the phase decomposition, the change of morphology should be another critical challenge because it happens at a relatively low temperature (even lower than 100 ℃)[12]. Considering that a relatively high working temperature is unavoidable for the outdoor use of the organic-inorganic perovskite solar cells due to the continuous sunlight illumination[13]. The changing morphology of the film results in varying electronic and physical contact between hole transporter-perovskite, hole transporter-TiO_2 layer, perovskite-TiO_2 layer, and even hole transporter-electrode, which highly restricts the device reproducibility and longtime stability[12]. The morphology evolution upon the annealing was attributed to the minimization of the surface energy[14]. However, there is no detailed investigation of the dependence of surface energy of the perovskite domains on the film fabrication method.

In this work, we explicitly investigated the thermal stability of solution processed perovskite thin films and devices. Perovskite thin films with various morphologies were fabricated by tuning the inorganic/organic ratio in the precursor solution. The morphology and crystallinity evolution of the as-fabricated perovskite films during thermal annealing were studied by scanning electron microscopy (SEM) and X-ray diffraction (XRD). UV–vis absorption spectrum and photoluminescence were used to monitor the perovskite crystallization process. We further fabricated planar structure solar cell devices and compared the thermal stability of the devices based on different perovskite films. Highly stable devices were fabricated based on perovskite thin films with moderate grain size and lattice orientation, which showed no degradation after annealing at 100 ℃ for 5 h. Meanwhile the power conversion efficiency (PCE) of the control device degraded more than 30 %. This finding provided general guidelines for the development of thermally stable perovskite solar cells.

2. Method

Fabrication of perovskite thin films and devices: We used the mixed lead method to tune the morphology of perovskite thin films. Perovskite precursors, PbI_2, $PbCl_2$ and MAI, were premixed at molar ratio of 6 : 1 : 9, 4 : 1 : 7, 2 : 1 : 5, 1 : 1 : 4, 1 : 2 : 7. The inorganic/organic ratio in these precursors were 1 : 1.3, 1 : 1.7, 1 : 2, 1 : 2.3, respectively. We dissolved the premixed precursors in N,N-Dimethylformamide (DMF) solution at a weight ratio of 40%. The conventional recipe of PbI_2 : MAI = 1 : 1 and $PbCl_2$: MAI = 3 : 1 were also prepared as the control group. To fabricate perovskite thin films, the precursor solutions were then spin-coated onto FTO glass with compact TiO_2 layer and annealed in Ar glovebox at 100 ℃ for 1 h. To fabricate PSC devices, 30 nm thick P3HT layer was spin-coated onto the perovskite layer, followed by thermal evaporation of 80 nm thick Ag electrode.

Thermal stability characterization of perovskite thin films and devices: X-ray diffraction (Bruker D8 advance X-ray

* Project supported by the Youth Innovation Promotion Association of CAS (No. 2015167).

† Corresponding author. Email: pangsp@qibebt.ac.cn, cuigl@qust.edu.cn

Received 23 August 2016, revised manuscript received 11 October 2016

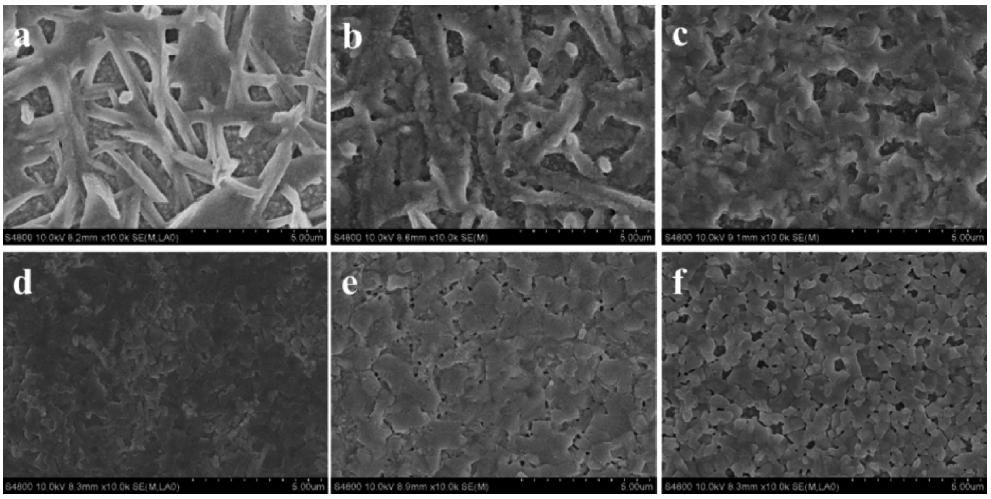

Fig. 1. Morphology evolution of perovskite films based on mixed lead precursor with different inorganic/organic ratio: (a) 1 : 1, (b) 1 : 1.3, (c) 1 : 1.7, (d) 1 : 2, (e) 1 : 2.3, (f) 1 : 3. The inorganic/organic ratio gradually decreased from (a) to (f).

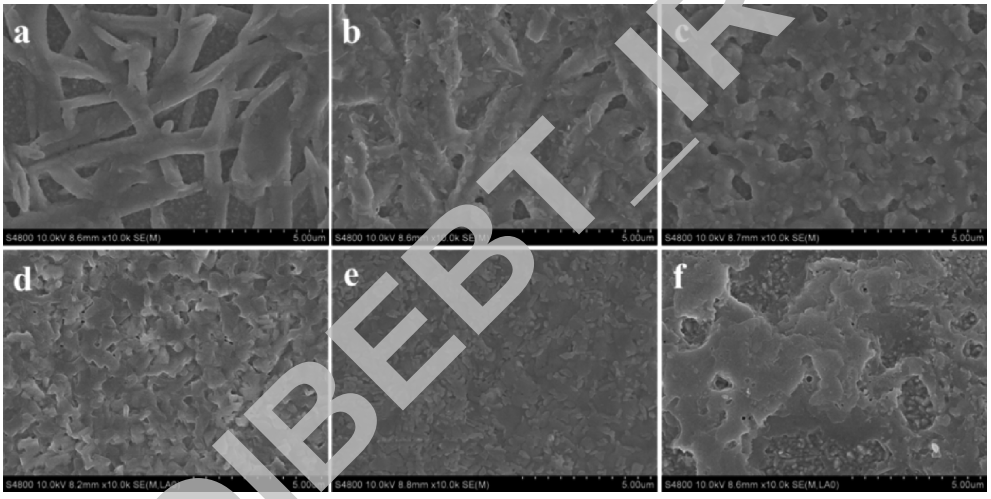

Fig. 2. Morphology evolution of perovskite films based on mixed lead precursor after 5 h annealing. (a)–(f) were the same sample as in Fig. 1.

diffractometer) and field-emission scanning electron microscopy (Hitachi S-4800) were used to characterize the morphology and crystallinity of perovskite thin films before and after prolonged annealing (5 h at 100 ℃ in air). UV–vis spectrometer (Hitachi U-4100) was used to characterize the absorption of perovskite thin film during thermal annealing. The current–voltage curves of the as-fabricated devices were measured (2400 Series Source Meter, Keithley Instruments) in air every 30 min during the prolonged annealing.

3. Result and discussion

3.1. Morphological stability of perovskite thin films

As shown in Fig. 1, the morphology of the as fabricated perovskite thin films changes gradually when we decrease the inorganic/organic ratio (Pb^{2+}/MA^{+} ratio) in the precursor solution step-by-step (Table 1). When the inorganic/organic ratio was high (sample a and b), the crystallization process of perovskite was quite fast and fiber-like perovskite grains were formed due to the strong coordination effect between Pb^{2+} and residue DMF molecules in the film[15, 16]. As the ratio went lower, excess organic component in the precursor film prevented the fast crystallization of perovskite. During thermal annealing, excess organic component needed to be slowly sublimated before perovskite crystallization[17, 18]. It took about 1 h for low inorganic/organic ratio samples to totally convert into perovskite. The existence of excess organic component also screened the coordination between Pb^{2+} and DMF, and thus eliminated the fiber-like structure. When the inorganic/organic ratio was 1/2 (Fig. 1(d)), uniform and pin-hole free perovskite thin films were fabricated.

It should be noted that for the conventional $PbCl_2$-based method, the as-fabricated perovskite thin films shrank during thermal annealing (sample f). The same phenomena were also observed in the sample with low inorganic/organic ratio (sample e). As we further annealed all the samples at 100 ℃ for 5 h, the shrinkage problem became more serious in the samples with low inorganic/organic ratio (Fig. 2). By comparing with Fig. 1, we could clearly see the effect of inorganic/organic ratio on the morphological stability of perovskite thin films. However, the samples with higher inorganic/organic ratio were rela-

Table 1. The relationship between inorganic/organic ratio and mixed lead precursor.

Sample	a	b	c	d	e	f
Inorganic/organic	1 : 1	1 : 1.3	1 : 1.7	1 : 2	1 : 2.3	1 : 3
PbI_2 : $PbCl_2$: MAI	1 : 0 : 1	6 : 1 : 9	2 : 1 : 5	1 : 1 : 4	1 : 2 : 7	0 : 1 : 3

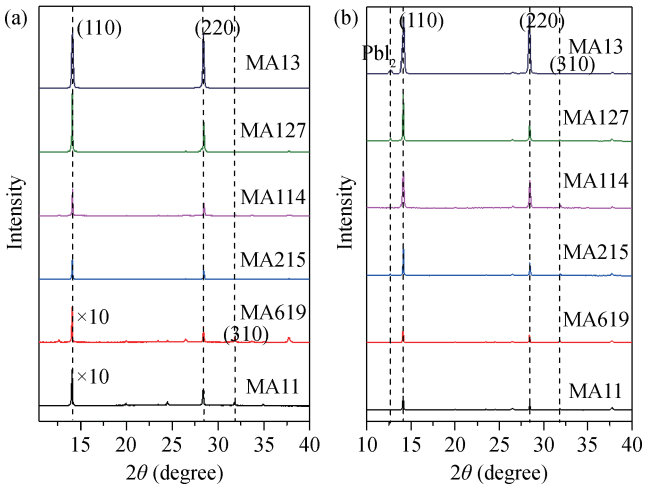

Fig. 3. XRD evolution of perovskite films based on mixed lead precursors, annealed for (a) 1 h and (b) 5 h.

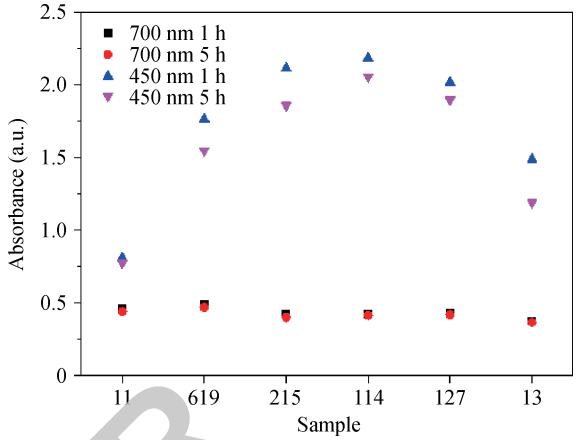

Fig. 4. UV absorbance of different perovskite samples at 450 and 700 nm wavelength, annealed for 1 and 5 h, respectively.

tively stable (samples a–d). For samples with inorganic/organic ratio higher than 1/2, the morphology remained unchanged during the prolonged annealing.

As we observed above, the inorganic/organic ratio in precursor solution had great influence on the morphology of as-fabricated perovskite thin film. We speculated that the morphological stability difference came from the different crystallization speed of perovskite, which resulted in different crystallinity of the film[19]. X-ray diffraction was performed on all the samples before and after prolonged annealing (Figs. 3(a), 3(b)). As shown in Fig. 3(a), the diffraction peaks at 14.08°, 28.40° and 31.86° could be assigned to (110), (220) and (310) diffractions of the tetragonal $MAPbI_3$ phase, in accordance with reported results[20]. This indicated that heating for an hour was enough for all the samples to sublimate the excess organic component and crystalize to perovskite. When the inorganic/organic ratio was high, the (310) peak was also relatively high (comparing with the (110) peak). However, as the inorganic/organic ratio decreased, the (310) peak could barely be seen and the (110) and (220) peak became extremely strong. This indicated that the grain orientation of the as-fabricated perovskite films was related to the inorganic/organic ratio in the precursor. Low inorganic/organic ratio samples had stronger grain orientation. Interestingly, the grain orientation evolution was in accordance with the morphological stability change. It is worth noting that we observed a new peak at 12.52° in sample f after prolonged annealing, which could be assigned to PbI_2. This indicated sample f decomposed during annealing. It seems that weak grain orientation was also in favor of better thermal stability.

Therefore, combining results from SEM and XRD, we concluded that the morphological stability of perovskite thin films was tightly related with the grain orientation in perovskite polycrystalline films. According to previous reports, perovskite crystals would rearrange to reduce surface energy during thermal annealing. Thus the samples with stronger grain orientation were more likely to shrink (Fig. 2(f)). However, for perovskite thin film with weak lattice orientation, grains need to shrink in different directions in order to lower their own surface energy. Therefore, the different grains restrict each other from shrinking and prevent the formation of large pin-holes.

However, if we took the device performance into consideration, strong grain orientation was undoubtedly important for fast charge transport and reduced charge recombination. Hence, there should be a balance between grain orientation and film shrinkage to promote device performance. Again, we chose sample d to be the most optimized sample because of the strong lattice orientation and high morphological stability.

To clarify the effect of the morphology evolution on the light absorption property, different perovskite samples were annealed for both 1 and 5 h . Sample d shows better absorption that typical PbI_2-based (sample a) or $PbCl_2$-based samples (sample f). The improvement was probably caused by the uniform and homogenous morphology and the formation of more compact crystal grains.

The absorption of all the samples showed a slight decline after the prolonged thermal treatment for 5 h. The decline mainly took place at wavelengths below 600 nm. However, there was no remarkable change in the shape of absorption curve at longer wavelength, indicating that this decline mainly came from the morphology change rather than the decomposition of perovskite. Therefore, the degree of decline in absorption could be more evidence for the perovskite thermal stability. As shown in Fig. 4, UV–vis absorption at 450 nm degraded more seriously than at 700 nm. Sample a showed the least degradation while sample f showed the most. This indicated that samples with stronger grain orientation suffered from more serious shrinkage.

The intensity of PL reflected the radioactive recombina-

Table 2. Detailed parameter extracted from Fig. 6.

Sample	V_{oc} (V)	J_{sc} (mA/cm^2)	FF (%)	Eff (%)
11	0.71	12.4	34	3.0
619	0.7	13.8	48	4.8
215	0.91	18.4	64	10.7
114	0.94	19.3	70	12.9
127	0.9	18.8	61	9.5
13	0.79	16.1	58	7.4

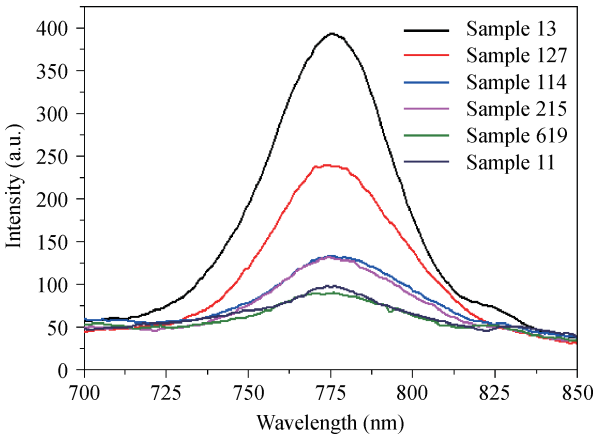

Fig. 5. (Color online) Photoluminescence of perovskite films based on mixed lead precursor.

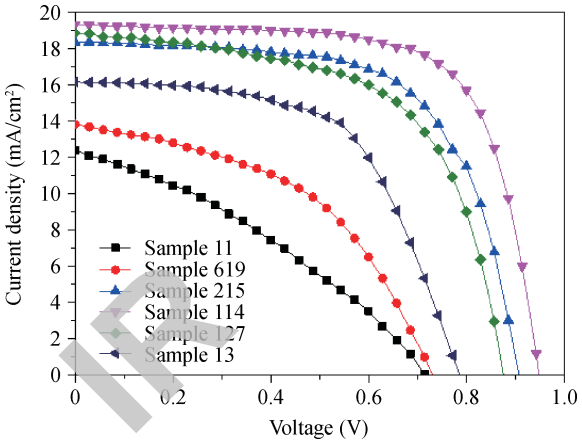

Fig. 6. (Color online) J–V curves of perovskite solar cells based on mixed lead precursor.

tion of photo-generated carriers in perovskite thin films. Typically, non-radioactive recombination were trap-assisted recombination, thus we usually expected films with more radioactive recombination to have better crystallinity and lower trap density[21]. For PL characterization, the perovskite films were directly spin coated on the insulting glass and annealed at 100 ℃ for 1 h. Since the films fabricated from all the samples had the same thickness, we roughly estimated the amount of radioactive recombination by the relative intensity of PL spectrum. As shown in Fig. 5, the intensity increased with the ratio of excess organic component in the precursor, indicating better crystallinity in these samples, which was in agreement with the XRD results. The absorption profile remained unchanged when tuning the inorganic/organic ratio, suggesting that no structural change happened in the perovskite films.

3.2. Thermal stability of perovskite solar cells

Solar cell devices were fabricated based on the as-fabricated perovskite thin films with a structure of FTO/compact TiO_2/Perovskite/P3HT/Ag. The J–V curves measured under AM 1.5 100 mW/cm^2 were shown in Fig. 6. Detailed data were presented in Table 2. The typical PbI_2-based sample (Sample a) showed the poorest performance of 3.0%. The low voltage resulted from the shunting pathway caused by the contact between P3HT and compact TiO_2 through the non-continuous perovskite film. The fill factor (FF) was also very low because of the serious carrier recombination. The introduction of excess organic component dramatically promoted cell performance. The performance increased while the inorganic/organic ratio gradually decreased from sample b to sample d. However, further decrease of the inorganic/organic ratio in the precursor degraded the performance, which resulted from the degraded morphological stability. Thus, considering both good crystallinity and high morphological stability, we thought sample d should be the best recipe. We further optimized the annealing temperature and perovskite thickness. The best performance of 12.9% was achieved based on the sample d, with an open circuit voltage (V_{oc}) of 0.94 V, a short circuit current (J_{sc}) of 19.3 and a FF of 70%.

The hysteresis between different voltage scan directions was related to the slow transient capacitive current, trapping and de-trapping process, ion migrations, and ferroelectric polarization within the perovskite layer, which had already been discussed in recent publications[22]. The solar cells based on sample d showed negligible hysteresis, which resulted from the better crystallinity, lower density of traps and more suitable film thickness which balanced the charge diffusion and light absorption.

In order to find out the influence of morphological stability on device performance, we directly annealed the devices at 100 ℃ in the oven for 5 h. The devices were measured every half an hour and the performance evolution was shown in Fig. 7. At the first half hour, the J_{sc} and FF slightly increased due to the slightly improved crystallinity of perovskite. The J_{sc} continued to increase in the next half hour but FF and V_{oc} typically remained the same. Then all the parameters including device efficiency were maintained during the thermal treatment, showing extraordinary thermal stability at 100 ℃. This was in good agreement with the high morphological stability of sample d observed by SEM (Fig. 1(d) and Fig. 2(d)). However, the performance of devices based on sample f degraded a lot dur-

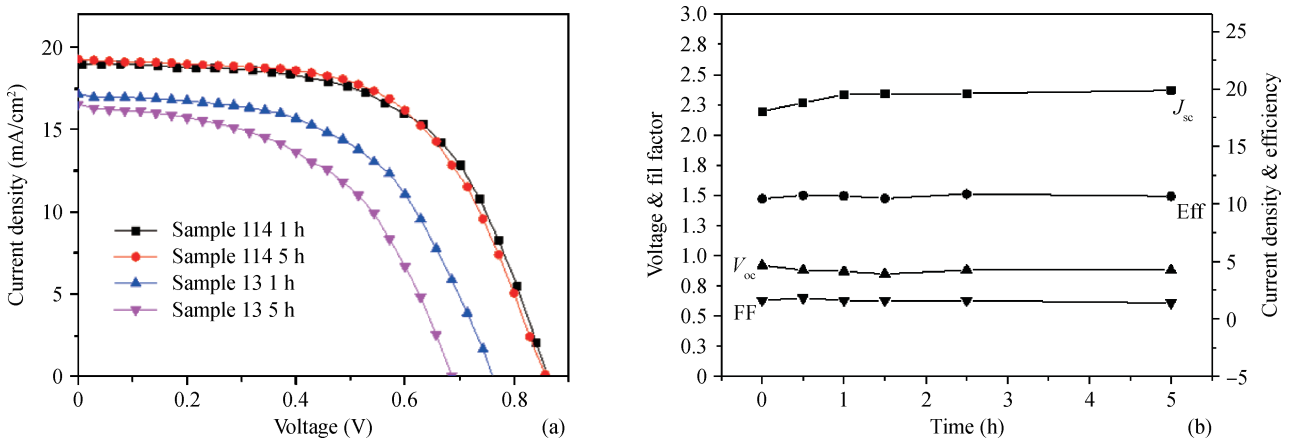

Fig. 7. (Color online) (a) Influence of morphological stability of perovskite films on device performance. (b) Thermal stability of perovskite devices based on sample 114.

ing prolonged annealing (Fig. 7(a)). The degradation resulted from the film shrinkage. As shown in Fig. 7(a) and (b), regardless of the annealing time of perovskite films, devices based on sample d showed similar performance, which was in agreement with the good morphological stability of sample d.

However, it should be noted that the perovskite layer is not the only layer affecting the thermal stability of devices. For example, we use the same technique to fabricate the devices but dope the hole transporting P3HT with 4-tert-butylpyridine (TBP, 2.9 mg/mL) and Li-TFSI (0.5 mg/mL). The devices show slightly higher efficiency than the undoped samples at the beginning. However, during the 5 h annealing at 100 ℃ in the oven, the V_{oc}, FF and the overall efficiency continue decreasing. This instability behavior may be caused by the sublimation of the dopant during thermal annealing, which still needs further investigation.

4. Conclusion

In summary, we systematically studied the thermal stability of both perovskite materials and perovskite solar cells. We employed the mixed lead method to fabricate $MAPbI_{3-x}Cl_x$ perovskite films and disclosed that the morphological stability of perovskite thin film was strongly related with the grain orientation, which could be tuned by the inorganic/organic ratio in precursor solution. Highly uniform and homogenous perovskite films can be fabricated by precursor solution with a molar ratio of PbI_2, $PbCl_2$ and MAI = 1 : 1 : 4. This was the optimized film which achieved a balance between strong grain orientation and good thermal stability. Devices based on mixed lead precursors confirmed the best performance of sample d as the highest efficiency reaching 14%. The as-fabricated devices showed extraordinary thermal stability during prolonged thermal treatment at 100 ℃ for 5 h. Moreover, this work focused on the thermal stability issues of perovskite solar cells for the first time and opened an avenue to fabricate thermally stable devices by employing feasible mixed lead method.

References

[1] Sum T C, Mathews N. Advancements in perovskite solar cells: photophysics behind the photovoltaics. Energy Environ Sci, 2014, 7(8): 2518
[2] Zuo C T, Bolink H J, Han H W, et al. Advances in perovskite solar cells. Adv Sci, 2016, n/a-n/a
[3] Boix P P, Nonomura K, Mathews N, et al. Current progress and future perspectives for organic/inorganic perovskite solar cells. Mater Today, 2014, 17(1): 16
[4] Stranks S D, Eperon G E, Grancini G, et al. Electron-hole diffusion lengths exceeding 1 micrometer in an organometal trihalide perovskite absorber. Science, 2013, 342(6156): 341
[5] Green M A, Emery K, Hishikawa Y, et al. Solar cell efficiency tables (Version 45). Prog Photovoltaics: Res Appl, 2015, 23(1): 1
[6] Lungenschmied C, Dennler G, Neugebauer H, et al. Flexible, long-lived, large-area, organic solar cells. Sol Energy Mater Sol Cells, 2007, 91(5): 379
[7] Krebs F C, Tromholt T, Jorgensen M. Upscaling of polymer solar cell fabrication using full roll-to-roll processing. Nanoscale, 2010, 2(6): 873
[8] Im J H, Lee C R, Lee J W, et al. 6.5% efficient perovskite quantum-dot-sensitized solar cell. Nanoscale, 2011, 3(10): 4088
[9] Kim H S, Lee C R, Im J H, et al. Lead iodide perovskite sensitized all-solid-state submicron thin film mesoscopic solar cell with efficiency exceeding 9%. Sci Rep, 2012, 2: 591
[10] Baikie T, Fang Y N, Kadro J M, et al. Synthesis and crystal chemistry of the hybrid perovskite $(CH_3NH_3)PbI_3$ for solid-state sensitised solar cell applications. J Mater Chem A, 2013, 1(18): 5628
[11] Dualeh A, Tétreault N, Moehl T, et al. Effect of annealing temperature on film morphology of organic-inorganic hybrid pervoskite solid-state solar cells. Adv Funct Mater, 2014, 24: 3250
[12] Eperon G E, Burlakov V M, Docampo P, et al. Morphological control for high performance, solution-processed planar heterojunction perovskite solar cells. Adv Funct Mater, 2014, 24(1): 151
[13] Aberle A, Dubey S, Sarvaiya J N, et al. Temperature dependent photovoltaic (pv) efficiency and its effect on pv production in the world—a review. Energy Procedia, 2013, 33: 311
[14] Wang Y, Sumpter B G, Huang J S, et al. density functional studies of stoichiometric surfaces of orthorhombic hybrid perovskite $CH_3NH_3PbI_3$. J Phys Chem C, 2015, 119(2): 1136
[15] Persson I, Lyczko K, Lundberg D, et al. Coordination chemistry study of hydrated and solvated lead (II) ions in solution and solid state. Inorg Chem, 2011, 50(3): 1058
[16] Zhou H P, Chen Q, Li G, et al. Interface engineering of highly

efficient perovskite solar cells. Science, 2014, 345(6196): 542
[17] Zhao Y X, Zhu K. CH_3NH_3Cl-assisted one-step solution growth of $CH_3NH_3PbI_3$: structure, charge-carrier dynamics, and photovoltaic properties of perovskite solar cells. J Phys Chem C, 2014, 118(18): 9412
[18] Wang D, Liu Z H, Zhou Z M, et al. Reproducible one-step fabrication of compact $MAPbI_{3-x}Cl_x$ thin films derived from mixed-lead-halide precursors. Chem Mater, 2014, 26(24): 7145
[19] Xiao Z G, Wang D, Dong Q F, et al. Unraveling the hidden function of a stabilizer in a precursor in improving hybrid perovskite film morphology for high efficiency solar cells. Energy Environ Sci, 2016, 9(3): 867
[20] Dong Q, Fang Y, Shao Y, et al. Electron-hole diffusion lengths > 175 μm in solution-grown $CH_3NH_3PbI_3$ single crystals. Science, 2015, 347(6225): 967
[21] Tress W, Marinova N, Inganäs O, et al. Predicting the open-circuit voltage of $CH_3NH_3PbI_3$ perovskite solar cells using electroluminescence and photovoltaic quantum efficiency spectra: the role of radiative and non-radiative recombination. Adv Energy Mater, 2015, 5(3): 1400812
[22] Chen B, Yang M J, Priya S, et al. Origin of J–V hysteresis in perovskite solar cells. J Am Chem Soc, 2016 7(5): 905